Supporting Information for "Two-Electron Oxygen Reduction on Carbon Materials Catalysts: Mechanisms and Active Sites"

Guo-Liang Chai,[*,†] Zhufeng Hou,[‡] Takashi Ikeda,[¶] and Kiyoyuki Terakura[‡,§]

†*State Key Laboratory of Structural Chemistry, Fujian Institute of Research on the Structure of Matter (FJIRSM), Chinese Academy of Sciences, Fuzhou, 350002 Fujian, People's Republic of China.*

‡*National Institute for Materials Science (NIMS), 1-2-1 Sengen, Tsukuba, Ibaraki 305-0047, Japan*

¶*Synchrotron Radiation Research Center, National Institutes for Quantum and Radiological Science and Technology (QST), 1-1-1 Kouto, Sayo, Hyogo 679-5148, Japan*

§*Research Center for Simulation Science, Japan Advanced Institute of Science and Technology (JAIST), 1-1 Asahidai, Nomi, Ishikawa 923-1292, Japan*

E-mail: g.chai@fjirsm.ac.cn

Hydrogenation energy calculation

The hydrogenation energies of different types of CMCs at zero temperature are calculated by the following equation:

$$\Delta E = E_{*\mathrm{H}} - E_{*} - \frac{1}{2}E_{\mathrm{H}_2}, \tag{S1}$$

where, the "*" denotes a CMC site and we take H_2 as the energy reference as in previous papers.[1,2] Thus, the hydrogenation energy corresponds to the reaction energy of the following reaction in the fuel cell:

$$* + (\mathrm{H}^{+}_{(\mathrm{aq})} + e^{-}) \rightarrow *\mathrm{H}. \tag{S2}$$

The calculated hydrogenation energy is the total energy, and this can be converted to the free energy by adding zero point energy, entropy, and solvation energy corrections as following:

$$\Delta G = \Delta E + \Delta ZPE - T\Delta S + \Delta G_s. \tag{S3}$$

The experimental zero point energy and entropy of the hydrogen gas are used as references.[1] The solvation energy added is -0.22 eV. All these correction terms are summarized in Table S1. The total corrections for C-H, O-H, and N-H bonds are 0.15, 0.17, and 0.17 eV, respectively. The free energies including these corrections are displayed in Table 1 of the main text.

Several local atomic structures along the graphene edge are shown in Figure S1. The hydrogenation energy was calculated for the specific H atoms labeled by numbers. For nitrogen doped edges, the edges with pyridinium N and OH termination are named E-pN-OH (c) and E-pN-OH-1 (d). For E-pN-OH-1, the "1" means one H is removed from edge OH site. The edges with graphitic N and OH termination are named E-gN-OH (a) and E-gN-OH-1 (b). The edge with pyridinium N and H termination is named E-pN-H (e). For un-doped edges, the edge with H termination is named E-H (f), and the edge with OH termination are named E-OH (g) and E-OH-1 (h). The calculated hydrogenation energies for the labeled H

are also displayed in the parentheses in Figure S1. In this study, the structures with a positive hydrogenation energy will not be investigated because it means that the hydrogenation is thermodynamically unstable. For the structures with negative hydrogenation energies, we select the H site with a larger hydrogenation energy as a candidate active site as it is easier to be removed. Thus, the H1 sites in E-pN-H (e) and E-H (f), and the H2 sites in E-pN-OH-1 (d), E-gN-OH-1 (b), and E-OH-1 (h) are selected for H_2O_2 formation study. The simulation boxes for estimating the H abstraction barrier by O_2 molecule are shown in Figure S2 for the E-gN-OH-1 structure.

Three types of mono-vacancies (MV) are studied as mentioned in the main text, that is, hydrogenated undoped MV (MV-3H and MV-4H), hydrogenated N doped MV (MV-1N1H and MV-1N3H), and hydrogenated N doped oxidized MV (MV-1N1O1H and MV-1N2O2H). The structures for different degree hydrogenation are shown in Figure S3. The hydrogenation energy for these structures are shown in Table S2. We can see that hydrogenation energy for the third H of undoped MV is too strong for H_2O_2 formation, while that of the fourth H is weak even for OOH^- mechanism. Therefore, MV-3H and MV-4H structures are selected for comparison. For N doped MV, hydrogenation energy for the third H is good for OOH^- mechanism. As MV-1N1H structure is a typical structure for graphene vacancy according to previous study,[3] this structure is also studied for comparison. As to N doped oxidized MV, its stability and phase diagram is investigated by previous paper.[4] For one O oxidized MV, the O is rather stable and presents ether structure. Only the N can be hydrogenated because the hydrogenation energy for ether O is positive. So, only MV-1N1O1H structure is selected here. For two O oxidized MV, the first H can be bonded to N site strongly and the second H bonded to O site is favorable for H_2O_2 formation. However, the third cannot continue to be added to MV (with positive hydrogenation energy). Thus, MV-1N2O2H structure is selected for H_2O_2 formation investigation.

Reaction mechanisms and limiting potential

Three reaction mechanisms are proposed in the main text. Those are the OOH^- mechanism, the OOH radical mechanism and the *ad*-O_2 mechanism. As shown in Figure 2 (b) in the main text, there are three elementary steps for the OOH^- ion mechanism:

$$* + (H^+_{(aq)} + e^-) \rightarrow *H, \tag{S4}$$

$$*H + e^- + O_{2(g)} \rightarrow * + OOH^-_{(aq)}, \tag{S5}$$

$$* + OOH^-_{(aq)} + H^+_{(aq)} \rightarrow * + H_2O_{2(aq)}. \tag{S6}$$

The reaction free energy of the overall reaction is -1.40 eV. The reaction free energy of the first step is the calculated hydrogenation energy ΔG_{*H}. That of the third step is constant and has an experimental value of -0.69 eV for the standard condition. For non-standard conditions, this value can be derived as described in the main text. The reaction free energy of the second step can be obtained accurately by subtracting the free energy variations of the other two steps from the total reaction energy. For an example, it is $(-1.40 + 0.69 - \Delta G_{*H})$ under the standard condition.

For the OOH radical mechanism presented in Figure 2 (a) in the main text, the four elementary steps are described by:

$$* + (H^+_{(aq)} + e^-) \rightarrow *H, \tag{S7}$$

$$*H + O_{2(g)} \rightarrow * + OOH_{(aq)}, \tag{S8}$$

$$* + (H^+_{(aq)} + e^-) \rightarrow *H, \tag{S9}$$

$$*H + OOH_{(aq)} \rightarrow * + H_2O_{2(aq)}. \tag{S10}$$

The reaction free energies for the first and third steps are the hydrogenation energy. The

experimental reaction free energy for the following reaction

$$(\mathrm{H}^+_{(\mathrm{aq})} + e^-) + \mathrm{O}_{2(\mathrm{g})} \rightarrow \mathrm{OOH}_{(\mathrm{aq})}, \tag{S11}$$

is 0.125 eV.[5] Therefore, the reaction free energy of the second step is given by $(-\Delta G_{*\mathrm{H}} + 0.125)$. As the overall reaction free energy is -1.40 eV, that of the fourth step is given by $(-1.40 - \Delta G_{*\mathrm{H}} - 0.125)$. Figure 3 (c) also give the *ad*-O_2 mechanism for comparison, which contains two elementary steps:

$$* + (\mathrm{H}^+_{(\mathrm{aq})} + e^-) + \mathrm{O}_{2(\mathrm{g})} \rightarrow *\mathrm{OOH}, \tag{S12}$$

$$*\mathrm{OOH} + (\mathrm{H}^+_{(\mathrm{aq})} + e^-) \rightarrow * + \mathrm{H}_2\mathrm{O}_{2(\mathrm{aq})}. \tag{S13}$$

The reaction free energy of the first step is given by (-4.92 + $\Delta G_{*\mathrm{OOH}}$) according to previous papers.[1,2,6] As the overall reaction free energy is -1.40 eV, the reaction free energy of the second step is (3.52 - $\Delta G_{*\mathrm{OOH}}$). The $\Delta G_{*\mathrm{OOH}}$ for metal free CMC is in the range around 3.40 eV to 4.60 eV.[6] Thus, the maximum limiting potential of 0.70 V can be obtained when $\Delta G_{*\mathrm{OOH}}$ is 4.22 eV.

The limiting potential is defined as:

$$U_{\mathrm{L}} = \mathrm{Min}_i[-\Delta G_i]/ne, \tag{S14}$$

where n is the number of electrons transferred for each electrochemical step (here $n = 1$ for the one-electron transfer step) and e is the elementary charge. The meaning of the r.h.s. of the above equation is to select the smallest $[-\Delta G_i]$ among the ORR elementary steps. The limiting potential is the highest potential where all of the electrochemical steps are downhill in free energy, which can be compared with the half-wave potential measured in experiments.[7]

Charge state of OOH group

The Mulliken charge for OOH group in E-pN-OH-1 and MV-1N2O2H structures are calculated and shown in Table S3. Here the valence-core interaction is described by Troullier-Martins pseudopotentials for all the elements. Self-interaction correction (SIC) is added to the ordinary DFT calculation for charge calculation according to a previous paper.[8] In the calculations, one electron is supplied from cathode for each structure. The OOH charge is calculated for two cases, that is, the water solution is in half density of water (HDW), normal density of water (NDW). All the structures are relaxed by MD simulations with SIC before charge calculation. The geometry structures for charge calculation are selected from the trajectory with relative low Kohn-Sham energy.

As shown in Table S3, the OOH charge is -0.36 and -0.42 for MV-1N2O2H in HDW and NDW, respectively. The OOH charge is -0.25 and -0.41 for E-pN-OH-1 in HDW and NDW, respectively. As the average charge on O^{2-} in water molecule is around -0.90, the charge on OOH group makes it behave as an OOH^- ion.

OOH^- ion mechanism with first reaction step as RDS

OOH^- ion mechanism with second reaction step as RDS is discussed in the main text. Here, we discuss the situation when the RDS of OOH^- ion mechanism is the first reaction step. In this case, the reaction rate of the second step is much faster than that of the first step. The produced *H by the first step is converted to OOH^- very quickly by the second step compared to the generation rate. The back reaction of the first step can be neglected as the concentration of *H now is rather small. Therefore, the OOH^- generation rate is determined by the first step and depletion rate is determined by the third step. According to the steady state approximation theory, the Eq. (10) in the main text can be rewritten as:

$$\frac{kT}{h} \cdot [\mathrm{H}^+] \cdot [*] \cdot e^{\frac{-\Delta_r^{\neq} G_1 - \beta_1 \cdot U}{kT}} = \frac{kT}{h} \cdot [\mathrm{OOH}^-] \cdot [\mathrm{H}^+] \cdot e^{\frac{-\Delta_r^{\neq} G_3}{kT}}, \tag{S15}$$

where $\Delta_r^{\neq}G_1$ is the reaction free energy barrier of the first step. Here, we employ the same BET coefficients as that for Pt surface (a=0.26 and b=0.50).[9] Therefore, $\Delta_r^{\neq}G_1 = 0.26 + 0.5\Delta G_{*\mathrm{H}}$. The concentration of active sites is $[*] = 4.24$ mol/L as employed in the main text. β_1 is asymmetry parameter for the first reaction step according to Butler-Volmer equation. Here, we use the value of $\beta_1 = 0.5$. Note here that it involved with a proton or electron transfer under electrode potential for inner or outer sphere electron transfer, respectively. For each case the electrode effect cannot be neglected. This is different from the situation in the main text that an neutral O_2 molecule is approaching the electrode for inner sphere electron transfer. Now, we can obtain the maximum limiting potential similar to Eq. (17) in the main text:

$$U_{\max} \approx 0.53 + 0.33\Delta G_{*\mathrm{H}} + \frac{2}{3}kT\ln([\mathrm{H}^+]). \tag{S16}$$

The potential versus RHE can be obtained by subtracting $kT\ln([\mathrm{H}^+])$:

$$U_{\max} \approx 0.53 + 0.33\Delta G_{*\mathrm{H}} - \frac{1}{3}kT\ln([\mathrm{H}^+]). \tag{S17}$$

The PH value for experiments mainly around 0-3. We employ PH=2 for following discussions. The free energy variations of the first two steps now can be rewritten as:

$$\Delta G_1 = \Delta G_{*\mathrm{H}} \tag{S18}$$

$$\Delta G_2 = -1.14 - 1.66\Delta G_{*\mathrm{H}} \tag{S19}$$

The maximum limiting potential can obtain is the crossing points of the two lines determined by these two equations. we find that the maximum limiting potential determined by the crossing point is 0.43 V.

N doped and undoped armchair edges for two-electron ORR

The structures of N doped and undoped armchair edges are shown in Figure S6. The corresponding hydrogenation energies are shown in Table S4 and Table S5. For N doped OH terminated armchair edge (A-pN-OH), the first H is unstable and easy to be removed. Here, we removed the H at O1 site which shows the highest hydrogenation energy. After the first H is removed, the hydrogenation energy for A-pN-OH-1 is too strong to precede two electron ORR, that is, -0.68 and -1.25 eV for O2 and N site, respectively. As the maximum potential for $2e^-$ ORR is 0.7 V, the N doped OH terminated armchair edges are not active for $2e^-$ ORR. For the undoped OH terminated armchair edge (A-OH-1), the hydrogenation energy is also too strong (-0.81 eV) for $2e^-$ ORR.

As to the N doped H terminated armchair edge (A-pN-H), the hydrogenation energy for N site is too weak while that for C1 and C2 sites are too strong for $2e^-$ ORR as shown in Table S5. For the undoped H terminated armchair edge (A-H), the hydrogenation energy for is also too strong for $2e^-$ ORR.

References

(1) Nørskov, J. K.; Rossmeisl, J.; Logadottir, A.; Lindqvist, L.; Kitchin, J. R.; Bligaard, T.; Jónsson, H. Origin of the Overpotential for Oxygen Reduction at a Fuel-Cell Cathode. *J. Phys. Chem. B* **2004**, *108*, 17886–17892.

(2) Calle-Vallejo, F.; Martinez, J. I.; Rossmeisl, J. Density functional studies of functionalized graphitic materials with late transition metals for oxygen reduction reactions. *Phys. Chem. Chem. Phys.* **2011**, *13*, 15639–15643.

(3) Hou, Z.; Wang, X.; Ikeda, T.; Terakura, K.; Oshima, M.; Kakimoto, M. Electronic structure of N-doped graphene with native point defects. *Phys. Rev. B* **2013**, *87*, 165401.

(4) Hou, Z.; Shu, D.; Chai, G.; Ikeda, T.; Terakura, K. Interplay between oxidized monovacancy and nitrogen doping in graphene. *J. Phys. Chem. C* **2014**, *118*, 19795–19805.

(5) Anderson, A. B.; Jinnouchi, R.; Uddin, J. Effective reversible potentials and onset potentials for O_2 electroreduction on transition metal electrodes: theoretical analysis. *J. Phys. Chem. C* **2013**, *117*, 41–48.

(6) Chai, G. L.; Hou, Z. F.; Shu, D. J.; Ikeda, T.; Terakura, K. Active sites and mechanisms for oxygen reduction reaction on nitrogen-doped carbon alloy catalysts: Stone-Wales Defect and Curvature Effect. *J. Am. Chem. Soc.* **2014**, *136*, 13629–13640.

(7) Viswanathan, V.; Hansen, H. A.; Rossmeisl, J.; Nørskov, J. K. Unifying the $2e^-$ and $4e^-$ reduction of oxygen on metal surfaces. *J. Phys. Chem. Lett.* **2012**, *3*, 2948–2951.

(8) VandeVondele, J.; Sprik, M. A molecular dynamics study of the hydroxyl radical in solution applying self-interaction-corrected density functional methods. *Phys. Chem. Chem. Phys.* **2005**, *7*, 1363–1367.

(9) Tripkovic, V.; Skulason, E.; Siahrostami, S.; Norskov, J. K.; Rossmeisl, J. The oxygen reduction reaction mechanism on Pt(111) from density functional theory calculations. *Electrochim. Acta.* **2010**, *55*, 7975–7981.

Table S1: The corrections for converting the total energies to the free energies for different bond types. Units are in eV.

Bond type	TS	ZPE	$\Delta ZPE - T\Delta S$
$1/2H_2$	0.21	0.14	-0.07
C-H	0.0040	0.30	0.30
O-H	0.0037	0.32	0.32
N-H	0.0083	0.33	0.32

Table S2: The hydrogenation energies for graphene mono-vacancies. Units are in eV.

	H^{1st}	H^{2nd}	H^{3rd}	H^{4th}
MV-nH	-1.85	-0.70	-1.79	-0.23
MV-1NnH	-1.01	-1.32	-0.40	–
MV-1N2OnH	-1.01	-1.01	-0.41	0.08

Table S3: The OOH group charge for E-pN-OH-1 and MV-1N2O2H structures. HDW and NDW mean that the structures are in half density of water (HDW), normal density of water (NDW), respectively.

	E-pN-OH-1	MV-1N2O2H
HDW	-0.25	-0.36
NDW	-0.41	-0.42

Table S4: hydrogenation energies (in eV) for A-pN-OH, A-pN-OH-1 and A-OH structures, respectively.

	O1-H	O2-H	N-H
A-pN-OH	1.48	0.67	0.49
A-pN-OH-1		-0.68	-1.25
A-OH-1	-0.81		

Table S5: hydrogenation energies (in eV) for A-pN-H and A-H structures, respectively.

	C1-H	C2-H	N-H
A-pN-H	-1.32	-1.90	0.38
A-H	-2.38		

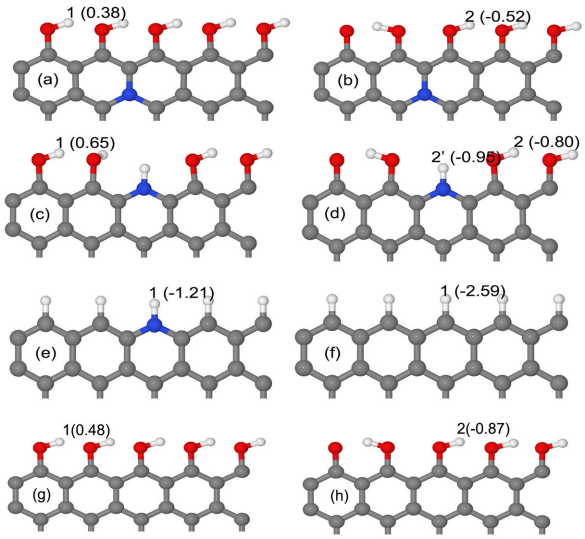

Figure S1: Local structures for different types of graphene edges and the hydrogenation energies for the specific H sites (in units of eV). Grey, blue, red and white balls represent carbon, nitrogen, oxygen and hydrogen atoms, respectively.

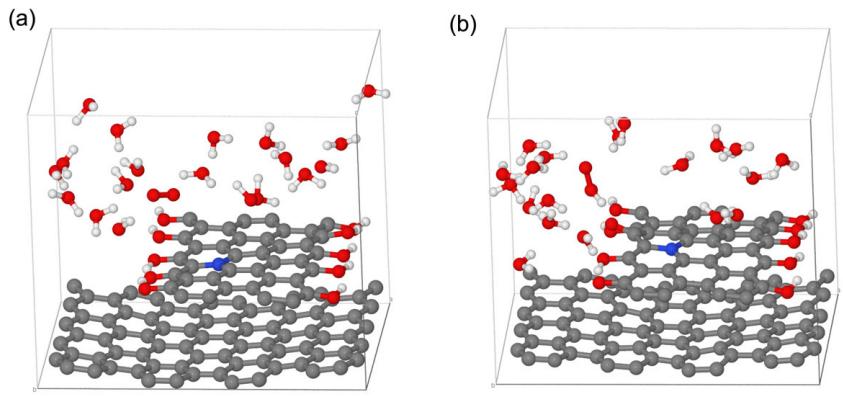

Figure S2: The initial and final structures for the abstraction of the edge H by an approaching O_2 molecule for the E-gN-OH-1 structure. Grey, blue, red and white balls represent carbon, nitrogen, oxygen and hydrogen atoms, respectively.

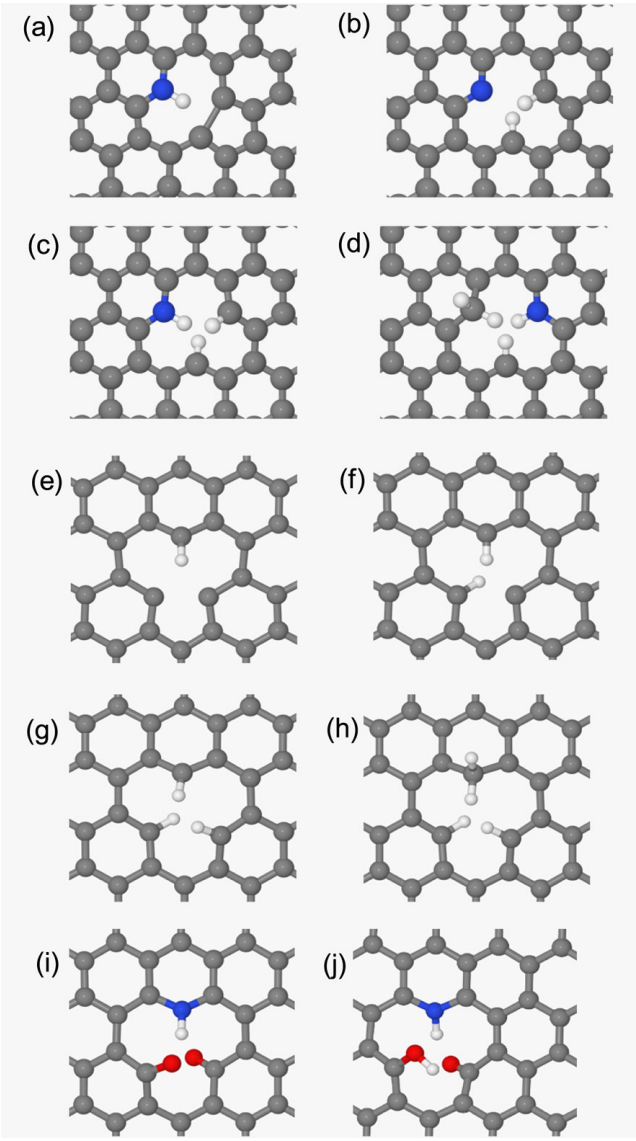

Figure S3: Local structures for different hydrogenation of graphene mono-vacancies: (a) MV-1N1H, (b) MV-1N2H, (c) MV-1N3H, (d) MV-1N4H, (e) MV-1H (f) MV-2H, (g) MV-3H, (h) MV-4H, (i) MV-1N2O1H and (j) MV-1N2O2H. Grey, blue, red and white balls represent carbon, nitrogen, oxygen and hydrogen atoms, respectively.

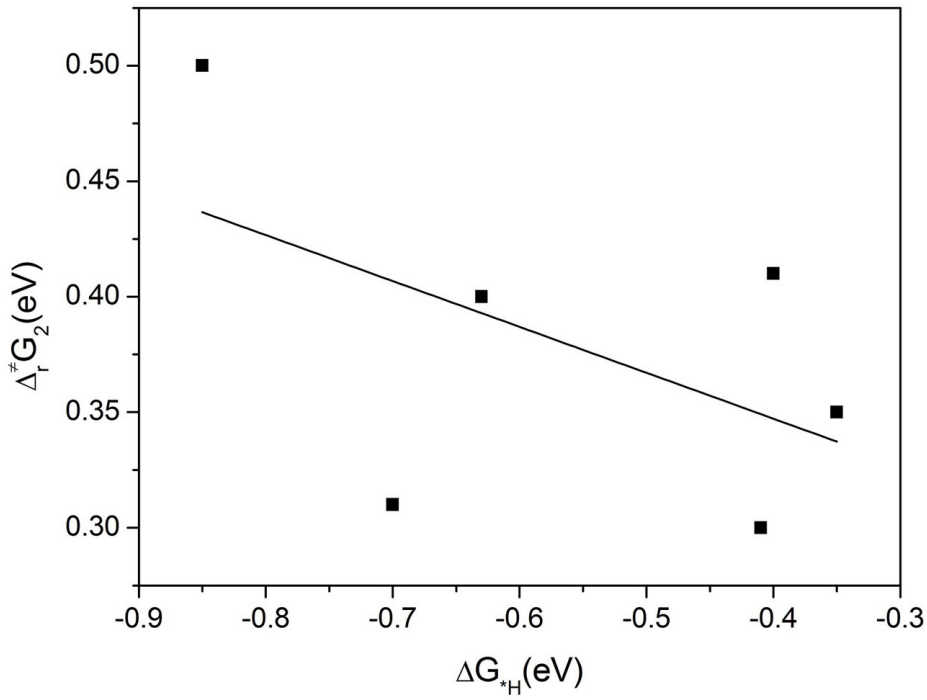

Figure S4: The fitting plot to obtain the values of a and b in Eq. 18 in the main text. The data of the structures with O_2 activation barriers lower than 0.6 eV are used.

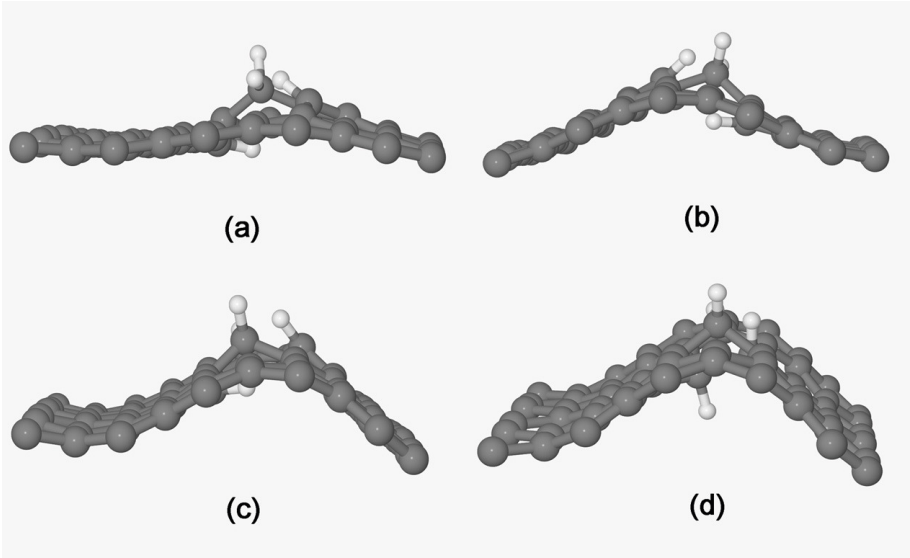

Figure S5: Structures for MV-4H with different strain/curvature: (a) 2.4%, (b) 6.5%, (c) 10.5%, (d) 14.6%. Grey and white balls represent carbon and hydrogen atoms, respectively.

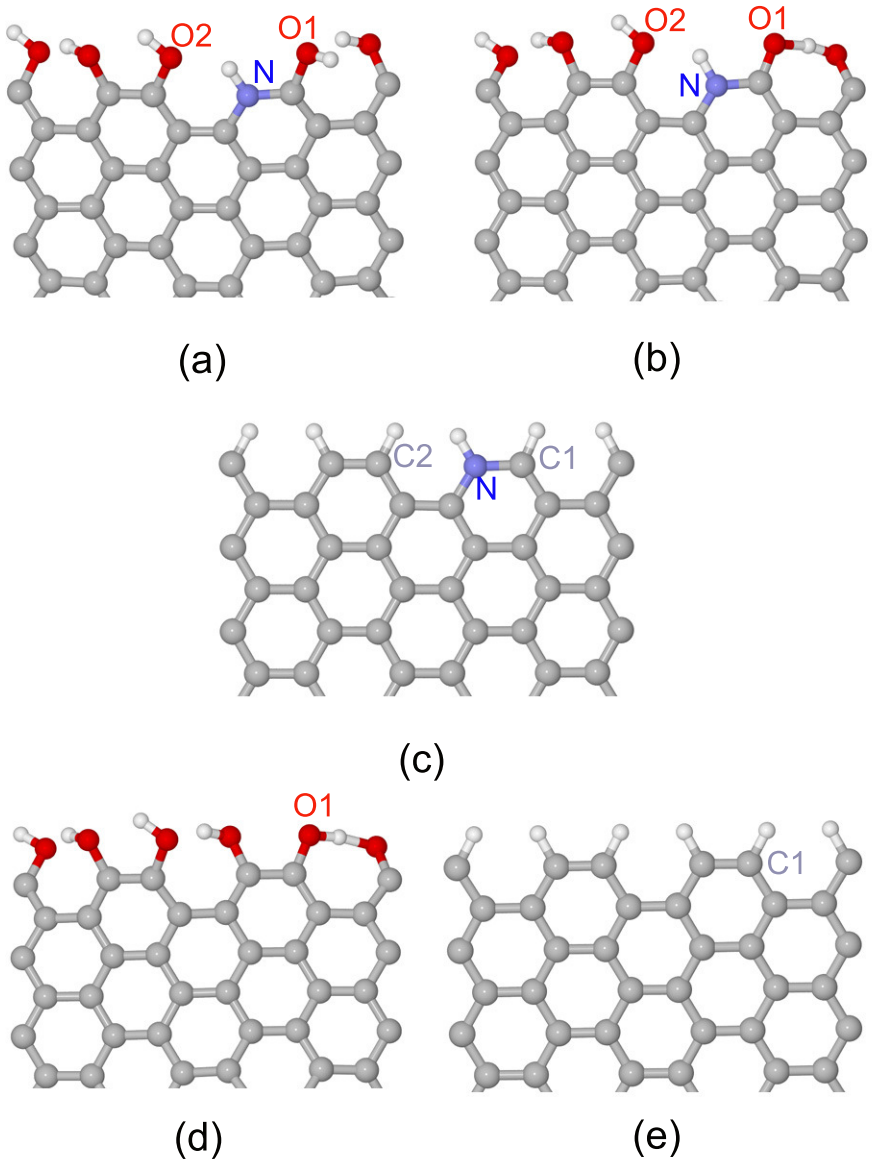

Figure S6: Local atomic structures of armchair edges. (a) A-pN-OH, (b) A-pN-OH-1, (c) A-pN-H, (d) A-OH-1, and (e) A-H. Grey, blue, red and white balls denote carbon, nitrogen, oxygen and hydrogen atoms, respectively.